Small Activity Differences Drive Phase Separation in Active-Passive Polymer Mixtures

Jan Smrek* and Kurt Kremer†
Max Planck Institute for Polymer Research, Ackermannweg 10, 55128 Mainz, Germany
(Received 17 October 2016; revised manuscript received 21 December 2016; published 1 March 2017)

Recent theoretical studies found that mixtures of active and passive colloidal particles phase separate but only at very high activity ratio. The high value poses serious obstacles for experimental exploration of this phenomenon. Here we show using simulations that when the active and passive particles are *polymers*, the critical activity ratio decreases with the polymer length. This not only facilitates the experiments but also has implications on the DNA organization in living cell nuclei. Entropy production can be used as an accurate indicator of this nonequilibrium phase transition.

DOI: 10.1103/PhysRevLett.118.098002

Active matter consists of microscopic constituents, such as bacteria, microswimmers, or molecular motors that transform energy from the surroundings or their own sources into mechanical work. The energy is fed into the system on the particle scale producing local spatiotemporal gradients which give rise to a number of interesting macroscopic nonequilibrium phenomena such as emergence of spatial structures through dynamical phase transitions [1], directed rotational motion [2], propagating waves [3,4], and phase separation of mixtures of active and passive particles with purely repulsive interactions [5–10].

The latter phenomenon, which we focus on here, is particularly interesting as often the active particles reside in a passive environment or the level of their activity is heterogeneous. Moreover, the mixture of active and passive polymers was hypothesized to play a role in the DNA organization within the cell nucleus during the interphase (metabolic phase of the cells life) [11–13]. Indeed, DNA transcription or the hypothesized active loop extrusion [14] involve continual energy influx and dissipation on microscopic length scales. Observations of living cells [15,16] and the "*C* experiments" [17] confirm that euchromatin—the active DNA, is colocalized and separated from the inactive denser heterochromatin by an unknown mechanism. The chemical difference of the hetero- and euchromatin [16] could play a role in the chromatin separation [18], and, as first shown by Ganai *et al.* [11], the active process that we are focusing on here too, could bring an additional contribution to the separation.

Recently, two works [6,10] modeled active colloidal particles as having higher diffusivity as their passive counterparts, by simply connecting them to a higher temperature thermostat. Both simulations and analytical theory predict phase separation at a temperature ratio of about 30. Similarly, high critical activity contrast is observed also for other, "vectorial" activity models such as active Brownian particles (ABP) [5] (Péclet number over 50) and Vicsek model [9,19], where the generated force or velocity acting on the particle has a specific direction that randomizes on longer time scales. These models are more complex due to other effects like pressure dependence on the interaction details of the particles with the container [20–22]. Thus, we here restrict ourselves to the simple but rich two temperature model and apply it to polymers. With the DNA application in target, the work [11] observed phase separation of partly active polymers, where some isolated monomers had temperature 20 times higher than the ambient one. Although hydrolysis of a single molecule of ATP releases energy of about $20k_BT$, this cannot be completely spent on the increase of the kinetic energy of the DNA. In any case, the factor of 20 or 30 of the critical activity contrast means, the active component in room temperature environment would have a temperature of about 10^4 K—certainly beyond a biologically relevant scale of intracellular processes.

However, the polymer degrees of freedom of the particles can play a crucial role in decreasing the critical activity ratio to relevant scales. It is well known that in *equilibrium* phase separation of *polymer* mixtures, the critical Flory interaction parameter, characterizing the asymmetry of the interaction between the two polymer species and driving their segregation, is inversely proportional to the polymer length N [23]. There, to leading order, the entropy, driving the mixing, is proportional to number of chains M, while the interaction, favoring the separation is proportional to MN, resulting in the $1/N$ dependence of the critical interaction parameter found in Flory-Huggins theory. Naturally, one asks: Is there an analogous effect in the active polymer matter? In other words, are for long (bio) polymers small activity differences sufficient to drive phase separation? This is what we set out to investigate.

To do so, we simulate monodisperse polymer melts of standard fully flexible and weakly semiflexible bead spring systems [24], detailed in the Supplemental Material [25], of $M = 1000$ chains of N beads that have been frequently used to investigate *equilibrium* properties of dense polymeric systems. We investigate systems of $N = 10$, 20, 40, 70, and 100 for flexible and additionally $N = 200$ for semiflexible chains at constant volume with bead density $\rho = 0.85\sigma^{-3}$

and periodic boundary conditions. Chains are effectively uncrossable and the entanglement length is $N_e \simeq 87$ in the flexible and $N_e \simeq 28$ in the semiflexible system [28]. To model activity differences, $M/2$ "cold" chains are coupled to a Langevin thermostat with temperature $T_c = 1.0\epsilon$ and the other "hot" chains to a Langevin thermostat with $T_h \geq T_c$. Each chain is either completely hot or cold, different from Refs. [29,30], where only the central monomer is active. The coupling with the thermostats is through friction coefficient γ. The choice of γ and the time step, besides the required stability of the simulation, is connected to the fact that the energy dissipation governed by γ is relevant for the specific interaction strength due to the heat transfer between the two species. Since we are here looking at the chain length effect only, one should use the same γ and time step for all the temperatures and chain lengths. This is satisfied by a rather high friction coefficient $\gamma = 10\tau^{-1}$ and a time step $\Delta t = 0.005\tau$. For comparison, the simulations in Ref. [6] used Brownian dynamics which corresponds to a high friction limit of molecular dynamics (MD) that we do here. All our simulations were performed using the ESPResSo++ simulation package [31]. As our polymers differ only by the thermostat, their phase separation and its behavior for different N is a pure nonequilibrium effect arising from their different kinetic properties (stiffness difference due to the temperature contrast is negligible—see the Supplemental Material [25]).

We start from well-mixed equilibrium configurations ($T_h = T_c$), then increase T_h and let the system evolve until a steady state is reached, typically at a time chains need to diffuse through the whole system. In the steady state: (i) For high T_h we find two liquids (as both components are well above the glass transition point) of different hot-cold composition. For temperatures close to the onset of segregation we observe slowing down of the evolution and large fluctuations (Fig. S1 in the Supplemental Material [25]). (ii) Comparison of semi- and fully flexible systems shows a small decrease in the critical temperature ratio with the stiffness of the polymers (Figs. 1 and 3). This is expected, as stiffer chains have a less-pronounced correlation hole (chain self-density), which leads to a slightly larger number of less favorable contacts [32]. (iii) Simulations of systems with different N (Fig. 3) exhibit the decrease of the temperature range of the transition with N.

In simple terms, separation emerges because hot particles exhibit larger effective excluded volume and "entrap" passive particles as illustrated in Ref. [6]. The hot particles exhibit higher pressure which is compensated by density change and phase separation [10,20]. Still the mixing tendency is present and some chains diffuse in both temperature regions.

Commonly, one tracks phase separation by an order parameter based on the normalized number difference of the hot and the cold beads, $\Phi_k = (n_{h,k} - n_{c,k})/(n_{h,k} + n_{c,k})$ in the kth subbox (see the Supplemental Material [25] for details). This is used in Fig. 1, where we plot $|\bar{\Phi}|(T_h)$, i.e., $|\Phi_k|$ averaged over all subboxes and over steady state

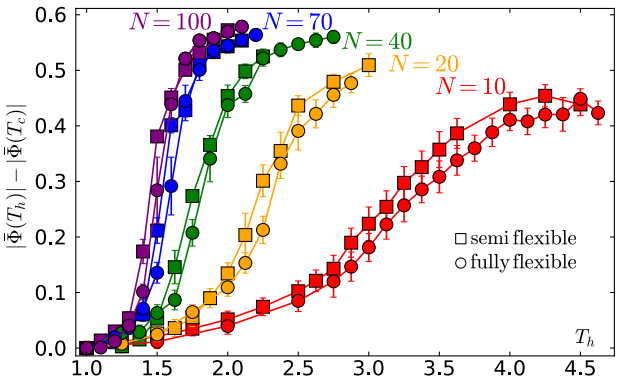

FIG. 1. Order parameter $|\bar{\Phi}|$ as function of T_h and N. A comparison of semiflexible (squares) and fully flexible (circles) chains shows systematically lower transition temperature for semiflexible polymers.

configurations and subtract $|\bar{\Phi}|(T_h = T_c)$ that is not exactly zero due to finite size effects. Since we lack a classical ensemble we cannot employ the usual semi-grand-canonical scheme of exchanging chain types, allowing one to evaluate the order parameter and higher order cumulants for the whole system [33–35]. This makes the Φ analysis suitable for trend description only. However, as we show below, the dependence of the critical temperature asymmetry on N can be determined more accurately from the entropy production rate.

Particles thermalize much faster than the composition of their local environment changes. Thus, both particle types have Maxwellian velocity distributions characterized by some effective temperatures T_h^{eff} and T_c^{eff} for hot and cold particles, respectively, where $T_h > T_h^{\text{eff}} > T_c^{\text{eff}} > T_c$, as shown in the inset of Fig. 2. This holds true for both the mixed *and* the phase separated systems (see Supplemental Material [25]). The values of the effective temperatures, the energy flux between the hot and cold subsystems and the related entropy production rate are determined by the local particle environment, reflecting the order of the system.

The Langevin thermostats act as reservoirs that pump energy to their respective subsystems by random force kicks and receive energy from them through the particle friction. The average power of the random force per hot particle is $\dot{E}_h^{\text{rand}} = -3\gamma T_h$ (we use units where $k_B = 1$) and similarly for the cold reservoir, where the minus sign follows our convention that the flux is positive when flowing *to* a reservoir. The friction force causes deceleration $\dot{\vec{v}} = -\gamma\vec{v}$ and, therefore, on average the related power per hot particle is $\dot{E}_h^{\text{fric}} = \gamma m\langle v_h^2\rangle = 3\gamma T_h^{\text{eff}}$. The average is taken only over the n_i particles connected to the thermostat i. In equilibrium, $T^{\text{eff}} = T$ and the energy flux due to random forces would be compensated by the friction. Out of equilibrium only the total power supplied to the system $-3\gamma(T_c n_c + T_h n_h)$ has to be balanced in steady state by the amount dissipated by the friction forces, i.e.,

$$-T_c - T_h + T_c^{\text{eff}} + T_h^{\text{eff}} = 0, \tag{1}$$

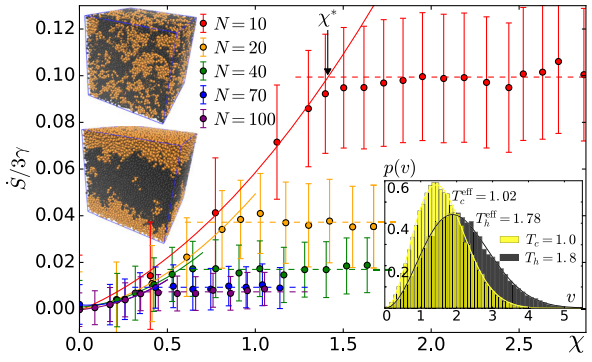

FIG. 2. Entropy production as an order parameter of the transition. Entropy production per hot particle in the steady state as function of N and $\chi=(T_h^{\rm eff}-T_c^{\rm eff})/T_c^{\rm eff}$ for flexible polymers. The solid colored lines are a quadratic fit to the low χ (mixed) regime the dashed colored lines are constant fit to the high χ (separated) regime. The black arrow shows the extracted critical value of χ for $N=10$ as the crossover point between the two regimes. Error bars represent ensemble standard deviations as described in the Supplemental Material [25]. Insets: Histograms—velocity distributions of the hot and cold particles in the separated state of $N=70$ and $T_h=1.8$, the effective temperatures are extracted as a fit of Maxwellian distribution. Two steady state $N=40$ system snapshots are shown: mixed (top) and phase separated (bottom) with hot chains (black) and cold chains (yellow).

because the system is not changing or producing work. Here and in what follows we used that our systems have equal number of hot and cold particles ($n_h=n_c$).

In steady state the entropy production rate (per hot particle) of each reservoir amounts to the net heat flux to the reservoir per hot particle $3\gamma(T_i^{\rm eff}-T_i)$ divided by the temperature of the reservoir T_i per unit time. The total entropy production of the system per hot particle $\dot{S}$ is the sum of the two contributions

$$\frac{\dot{S}}{3\gamma}=\frac{T_h^{\rm eff}}{T_h}+\frac{T_c^{\rm eff}}{T_c}-2. \tag{2}$$

The entropy production is always non-negative (equal to zero in equilibrium $T_h=T_c$), which follows from the temperature inequality and the power balance (1).

The analogue of the Flory interaction parameter is, in our case, the asymmetry of the *effective* temperatures $\chi=(T_h^{\rm eff}-T_c^{\rm eff})/T_c^{\rm eff}$ in the steady state. The effective temperatures control the particles' average kinetic and steric properties and therefore we choose χ over the thermostat temperature difference $dT=T_h-T_c$ (see also the Supplemental Material [25] for analysis in terms of dT). Moreover, because of finite friction γ, a small dT could lead to indistinguishable effective temperatures and the system would have no means to separate. Additionally, as the transition is governed by the effective temperature difference, the choice of friction should not have a strong effect on the transition position in terms of χ, as opposed to dT.

The entropy production per hot particle in the steady state increases with χ, due to the growth of the heat flux, until χ^*, above which it plateaus as the interface between the phases develops (Fig. 2). Therefore, the critical activity ratio χ^* (symbols in Fig. 3) is extracted as a crossover point between these two regimes. By phase separation, the hot chains maintain higher effective temperature by avoiding contacts with the cold chains, thus reducing the entropy production.

As the entropy production per particle is an average quantity over all the particles it has the advantage over the simple estimate from the number difference as it is not affected by the finite size effects of the artificial division of the simulation box. On the other hand, in the separated regime, the entropy production in small systems is dominated by the interface and therefore the plateau value depends on the system size. In the infinite system size limit, the interface contribution vanishes and the entropy production per particle will be governed by the finite fraction of the hot chains interspersed in the cold phase (and vice versa). But even in the thermodynamic limit the critical activity ratio would still be the crossover between two regimes (see Supplemental Material [25]). To quantify the interface effect, in the Supplemental Material [25] we compare the entropy production per particle for two different system sizes and find that although the effect is relevant, the shift in the critical activity ratio is within our temperature precision. To overcome the difficulties, rather than going to larger system sizes, it would be highly desirable to invent a method similar to the semi-grand-canonical scheme for equilibrium phase transition. This we leave for future work.

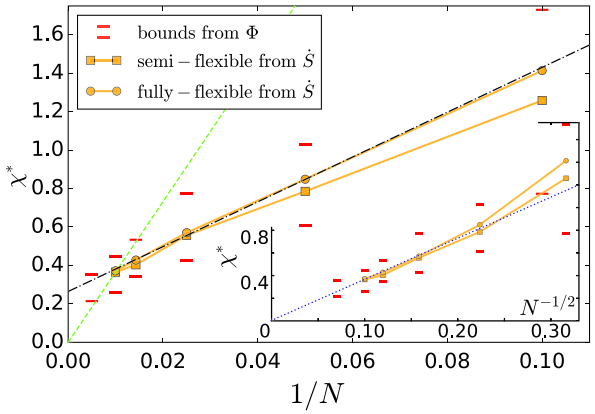

FIG. 3. Critical activity ratio as a function of the polymer length. Critical activity ratio χ^* is plotted as a function of $1/N$ for semiflexible (squares) and fully-flexible (circles) chains. Red marks delimit the range of the largest gradient of order parameter $|\bar{\Phi}|$ extracted from Fig. 1 (Supplemental Material [25]), symbols represent χ^* extracted from the entropy production rate $\dot{S}$ (see text). For $N=200$, the chains typically diffused only half of the box size; thus, did not completely reach a steady state for all χ. Based on the time profile of $|\Phi|$ (Fig. S2 in the Supplemental Material [25]) we marked the expected range of χ^*. The green dashed line connects the origin with the point χ^* at $N=100$, the black dot-dashed line is a linear function with an offset. Inset: the same data are plotted as a function of $1/N^{1/2}$, the blue-dotted line connects the origin with the point χ^* at $N=100$.

In analogy to equilibrium phase separation, there is a competition between the tendency to mix arising from the heat baths proportional to the number of chains and the tendency to avoid unfavorable contacts proportional to the number of monomers; thus, one could expect $\chi^* \sim 1/N$, i.e., $\chi^* N = \text{const}$. Interestingly, our data (Fig. 3) are not perfectly consistent with this trend. We approximately observe a linear $(1/N)$ regime, but the extrapolation leads to a nonzero χ^* at infinite N. This would mean that for infinitely long polymers one needs a finite difference of effective temperatures to drive segregation, which seems counterintuitive. In the inset of Fig. 3 we plot the same data of χ^* as function of $N^{-1/2}$, which agrees with the trend for the longest chain lengths as well as the expected infinite chain length limit. There are several possible explanations for this observation: (i) Finite size effects and nucleation: Even for our relatively large systems the effect of the interface has a relevant contribution to the entropy production in the separated regime (see Supplemental Material [25]) and one can expect the offset to decrease in the infinite system size limit. Moreover, at constant χN but very small χ, nucleation processes might be necessary for the separation to occur [6]. However, the velocity distributions overlap strongly at low χ and only a small fraction of hot particles is significantly hotter than the cold particles. Therefore, their nucleation becomes unlikely, especially when the total number of particles is limited. (ii) Mixing tendency grows with χ: The work [10] found for low densities that the separation of a system of spherical particles is governed by a free energylike function with a term that favors mixing but grows with χ. In other words, unlike in equilibrium phase transition, χ does not govern the separation tendency only. (iii) Critical phase composition depends on χ (even for 50:50 mixture). In equilibrium phase transition with *symmetric* interactions (i.e., interactions between like types of polymers are the same), the phase diagram is symmetric around the critical point located at the composition $1/2$ [23]. However, here the hot and cold phase have slightly different densities depending on χ. At different N, we probe different temperature ranges (and partial densities) and, therefore, we look at a binodal at slightly different relative volume fractions. However, for equilibrium phase transition this effect should decrease the apparent χ_c (see Supplemental Material [25]). The asymmetry causes that our 50:50 mixture likely probes the critical point only in the limit of $N \to \infty$, which also raises metastability issues. We briefly tested this for $N = 40$ (see Ref. [25]) and found the metastable region to be smaller than our temperature resolution. For longer chains, however, this might be different.

The reduction of the entropy production rate in the separated state is interesting in the context of the minimum entropy production principle [36]. This, however, is applicable close to equilibrium only, while in our case the temperature differences and gradients take place on the particle scale and, therefore, can be quite large. Thus, it would be interesting to look at much longer chains, and other models of activity especially Active-Ornstein-Uhlenbeck Particles (AOUP) [37], where one controls the distance from equilibrium by persistence time characterizing the velocity autocorrelation. For small persistence times one can define an effective temperature in a *pure* AOUP system [38] and it exhibits vanishing entropy production [37]. Therefore, it would be very interesting to see if the entropy production description also applies to passive-AOUP *mixtures* or to what extent this would be violated by the non-Boltzmann distribution of the AOUPs. Another interesting and possibly relevant extension would be to incorporate velocity correlations along the chain [39].

Consistent with symmetry considerations (Supplemental Material [25]), our data suggest that the entropy production scales as $\dot{S} \sim \gamma \chi^2 MN$ for small χ. Entropy produced on the relevant microscopic time scale γ^{-1}, i.e., $S \sim \chi^2 MN$ competes with the mixing entropy proportional to TM only. Here, for small enough χ the constant T should be close to average thermostat temperature and independent of χ. If this applies, it results in $\chi^* \sim N^{-1/2}$ scaling consistent with our results.

Our computational study uncovers a novel effect in the activity-driven phase separation. The strong decrease of the critical activity with the length of the polymers makes the active process relevant in the chromatin (self)organization, thus bridging the structure with the genome function. Moreover, it facilitates the experimental exploration in artificial systems like Ref. [40] and could pave a way for new polymeric active materials. Already the present simplest model opens a fascinating branch in polymer physics, and allows one to use its tools to search for and understand new phenomena out of equilibrium.

We would like to thank Burkhard Dünweg, Kostas Daoulas, Tristan Bereau, Cristina Greco, Horacio Vargas, Torsten Stuehn, and Alexander Grosberg for stimulating discussions. This work has been supported by the European Research Council under the European Union's Seventh Framework Programme (FP7/2007-2013)/ERC Grant Agreement No. 340906-MOLPROCOMP. We are grateful to the Max Planck Computing and Data Facility (MPCDF)

*smrek@mpip-mainz.mpg.de
†kremer@mpip-mainz.mpg.de

[1] J. Palacci, S. Sacanna, A. P. Steinberg, D. J. Pine, and P. M. Chaikin, Living crystals of light-activated colloidal surfers, Science **339**, 936 (2013).
[2] R. Di Leonardo, L. Angelani, D. Dell'Arciprete, G. Ruocco, V. Iebba, S. Schippa, M. P. Conte, F. Mecarini, F. De Angelis, and E. Di Fabrizio, Bacterial ratchet motors, Proc. Natl. Acad. Sci. U.S.A. **107**, 9541 (2010).
[3] V. Schaller, C. Weber, C. Semmrich, E. Frey, and A. R. Bausch, Polar patterns of driven filaments, Nature (London) **467**, 73 (2010).
[4] B. Szabó, G. J. Szöllösi, B. Gönci, Z. Jurányi, D. Selmeczi, and T. Vicsek, Phase transition in the collective migration of

tissue cells: Experiment and model, Phys. Rev. E **74**, 061908 (2006).
[5] J. Stenhammar, R. Wittkowski, D. Marenduzzo, and M. E. Cates, Activity-Induced Phase Separation and Self-Assembly in Mixtures of Active and Passive Particles, Phys. Rev. Lett. **114**, 018301 (2015).
[6] S. N. Weber, C. A. Weber, and E. Frey, Binary Mixtures of Particles with Different Diffusivities Demix, Phys. Rev. Lett. **116**, 058301 (2016).
[7] J. Denk, L. Huber, E. Reithmann, and E. Frey, Active Curved Polymers Form Vortex Patterns on Membranes, Phys. Rev. Lett. **116**, 178301 (2016).
[8] J. L. Silverberg, M. Bierbaum, J. P. Sethna, and I. Cohen, Collective Motion of Humans in Mosh and Circle Pits at Heavy Metal Concerts, Phys. Rev. Lett. **110**, 228701 (2013).
[9] B. Trefz, S. K. Das, S. A. Egorov, P. Virnau, and K. Binder, Activity mediated phase separation: Can we understand phase behavior of the nonequilibrium problem from an equilibrium approach?, J. Chem. Phys. **144**, 144902 (2016).
[10] A. Y. Grosberg and J.-F. Joanny, Nonequilibrium statistical mechanics of mixtures of particles in contact with different thermostats, Phys. Rev. E **92**, 032118 (2015).
[11] N. Ganai, S. Sengupta, and G. I. Menon, Chromosome positioning from activity-based segregation, Nucleic Acids Res. **42**, 4145 (2014).
[12] A. Awazu, Segregation and phase inversion of strongly and weakly fluctuating Brownian particle mixtures and a chain of such particle mixtures in spherical containers, Phys. Rev. E **90**, 042308 (2014).
[13] A. Y. Grosberg, Extruding loops to make loopy globules?, Biophys. J. **110**, 2133 (2016).
[14] A. Goloborodko, and J. F. Marko, and L. A. Mirny, Chromosome compaction by active loop extrusion, Biophys. J. **110**, 2162 (2016).
[15] T. Cremer, M. Cremer, B. Hbner, H. Strickfaden, D. Smeets, J. Popken, M. Sterr, Y. Markaki, K. Rippe, and C. Cremer, The 4D nucleome: Evidence for a dynamic nuclear landscape based on co-aligned active and inactive nuclear compartments, FEBS Lett. **589**, 2931 (2015).
[16] I. Solovei, K. Thanisch, and Y. Feodorova, How to rule the nucleus: divide et impera, Curr. Opin. Cell Biol. **40**, 47 (2016).
[17] E. Lieberman-Aiden, N. L. van Berkum, L. Williams, M. Imakaev, T. Ragoczy, A. Telling, I. Amit, B. R. Lajoie, P. J. Sabo, M. O. Dorschner, R. Sandstrom, B. Bernstein, M. A. Bender, M. Groudine, A. Gnirke, J. Stamatoyannopoulos, L. A. Mirny, E. S. Lander, and J. Dekker, Comprehensive mapping of long-range interactions reveals folding principles of the human genome, Science **326**, 289 (2009).
[18] D. Jost, P. Carrivain, G. Cavalli, and C. Vaillant, Modeling epigenome folding: formation and dynamics of topologically associated chromatin domains, Nucleic Acids Res. **42**, 9553 (2014).
[19] T. Vicsek, A. Czirók, E. Ben-Jacob, I. Cohen, and O. Shochet, Novel Type of Phase Transition in a System of Self-Driven Particles, Phys. Rev. Lett. **75**, 1226 (1995).
[20] A. P. Solon, Y. Fily, A. Baskaran, M. E. Cates, Y. Kafri, M. Kardar, and J. Tailleur, Pressure is not a state function for generic active fluids, Nat. Phys. **11**, 673 (2015).
[21] M. Kardar, Pressure from non-equilibrium fluctuations, talk at KITP Santa Barbara, 2016, http://online.kitp.ucsb.edu/online/sheets16/kardar/.
[22] N. Nikola, A. P. Solon, Y. Kafri, M. Kardar, J. Tailleur, and R. Voituriez, Active Particles with Soft and Curved Walls: Equation of State, Ratchets, and Instabilities, Phys. Rev. Lett. **117**, 098001 (2016).
[23] M. Rubinstein and R. Colby, *Polymer Physics* (Oxford University Press, Oxford, 2003).
[24] K. Kremer and G. S. Grest, Dynamics of entangled linear polymer melts: A molecular-dynamics simulation, J. Chem. Phys. **92**, 5057 (2016).
[25] See Supplemental Material at http://link.aps.org/supplemental/10.1103/PhysRevLett.118.098002 for further details on the simulation setup and the performed analysis, which includes Refs. [26,27].
[26] A. J. Liu and G. H. Fredrickson, Influence of nematic fluctuations on the phase separation of polymer blends, Macromolecules **25**, 5551 (1992).
[27] D. J. Kozuch, W. Zhang, and S. T. Milner, Predicting the Flory-Huggins χ parameter for polymers with stiffness mismatch from molecular dynamics simulations, Polym. Adv. Technol. **8**, 241 (2016).
[28] L. A. Moreira, G. Zhang, F. Müller, T. Stuehn, and K. Kremer, Direct equilibration and characterization of polymer melts for computer simulations, Macromolecular Theory Simul. **24**, 419 (2015).
[29] D. Loi, S. Mossa, and L. F. Cugliandolo, Effective temperature of active complex matter, Soft Matter **7**, 3726 (2011).
[30] D. Loi, S. Mossa, and L. F. Cugliandolo, Non-conservative forces and effective temperatures in active polymers, Soft Matter **7**, 10193 (2011).
[31] J. D. Halverson, T. Brandes, O. Lenz, A. Arnold, S. Bevc, V. Starchenko, K. Kremer, T. Stuehn, and D. Reith, ESPResSo++: A modern multiscale simulation package for soft matter systems, Comput. Phys. Commun. **184**, 1129 (2013).
[32] Y.-J. Sheng, A. Z. Panagiotopoulos, and S. K. Kumar, Effect of chain stiffness on polymer phase behavior, Macromolecules **29**, 4444 (1996).
[33] H.-P. Deutsch and K. Binder, Simulation of first- and second-order transitions in asymmetric polymer mixtures, Makromolekulare Chemie. Macromolecular Symposia **65**, 59 (1993).
[34] G. S. Grest, M. Lacasse, K. Kremer, and A. M. Gupta, Efficient continuum model for simulating polymer blends and copolymers, J. Chem. Phys. **105**, 10583 (2016).
[35] K. Binder and D. Heermann, *Monte Carlo Simulation in Statistical Physics* (Springer-Verlag, New York, 1988).
[36] I. Prigogine, *Etude Thermodynamique des Phenomènes Irrevérsibles* (Editions Desoer, Lieège, 1947), Chap. 5.
[37] E. Fodor, C. Nardini, M. E. Cates, J. Tailleur, P. Visco, and F. van Wijland, How Far from Equilibrium Is Active Matter?, Phys. Rev. Lett. **117**, 038103 (2016).
[38] U. Marini Bettolo Marconi and C. Maggi, Towards a statistical mechanical theory of active fluids, Soft Matter **11**, 8768 (2015).
[39] A. Suma, G. Gonnella, G. Laghezza, A. Lamura, A. Mossa, and L. F. Cugliandolo, Dynamics of a homogeneous active dumbbell system, Phys. Rev. E **90**, 052130 (2014).
[40] A. V. Ivlev, J. Bartnick, M. Heinen, C.-R. Du, V. Nosenko, and H. Löwen, Statistical Mechanics where Newton's Third Law is Broken, Phys. Rev. X **5**, 011035 (2015).